ELSEVIER

S0032-3861(96)00588-5

Polymer Vol. 38 No. 4, pp. 903–912, 1997

0032-3861/97/$17.00 + 0.00

Photoisomerization of a dye-altered β-1,4 glucan sheet induces the crystallization of a cellulose-composite

Susan K. Cousins and R. Malcolm Brown, Jr*
Department of Botany, University of Texas, Austin, TX 78713-7640, USA
(Received 20 January 1996; revised 6 May 1996)

Dye-altered β-1,4 glucan sheets synthesized by the bacterium *Acetobacter xylinum* in the presence of the fluorescent brightener Tinopal LPW™ were induced to crystallize into cellulose microfibrils by a novel photoisomerization of the dye molecules. Reducing the rate of dye removal led to more uniform microfibril dimensions, narrower ribbon width, and a greater microfibril helical pitch. The induced microfibrils are theorized to represent a composite of parallel glucan chains with dye molecules intercalated and deforming the cellulose lattice. It is speculated that during cellulose synthesis in general, glucan minisheets could associate by a constriction in the extrusion pore of the cellulose synthase complexes.

(Keywords: *Acetobacter xylinum*; cellulose composite; Tinopal LPW™)

INTRODUCTION

Cellulose synthesized from *Acetobacter xylinum* is an organized, twisting ribbon of microfibril bundles arising in close association with the bacterial envelope[1,2]. Cellulose biosynthesis in *Acetobacter* may be divided into two separate, successive steps[3,4]: (1) an enzymatically controlled polymerization of glucose residues and, (2) a cell-directed crystallization of the glucan chains. The polymerization of glucose residues occurs at the cytoplasmic membrane from catalytic sites located within enzyme complexes that span the bacterial envelope[5]. These enzyme complexes are arranged in a linear array of particles organized parallel to the long axis of the cell[1,2,6,7]. The array is known as a terminal complex (TC), and each particle is called a TC subunit.

The stages of crystallization (*Figure 1*) are manifested as a hierarchically arranged self-assembly process. Conflicting and confusing terminologies[8–12] have been used to describe the different levels of this hierarchy, so the nomenclature used in this paper is outlined in *Table 1*. In *Acetobacter xylinum*, the top of the hierarchy is represented by a ribbon of cellulose which extends parallel to the longitudinal axis of the cell[1] and is the result of the linear TC organization. Its constituent microfibrillar bundles each are composed of several microfibrils[12]. The microfibrillar bundles have been shown to be disrupted in cellulose synthesized in the presence of water-soluble cellulose derivatives, such as carboxymethylcellulose (CMC)[12], as well as by parabolic flight in microgravity studies[13]. Furthermore, these bundles are believed to form because the linear array of TC subunits is slightly discontinuous, as shown by freeze fracture[12]. Microfibrils, shown to be the true crystallites[14], are believed to form by the association of several minicrystals, which are evident when crystallization of cellulose is disrupted by addition of dyes[4]. Each TC subunit produces a single minicrystal comprised of approximately 10–16 glucan chains[15]. The minicrystals are theorized to form by the hydrogen bonding of van der Waals associated glucan mini-sheets[16]. Each catalytic site in a TC subunit is assumed to polymerize a single glucan chain[17].

One productive approach in understanding cellulose crystallization has been to alter the product during synthesis. This alteration has been accomplished by the incorporation of various direct dyes and fluorescent brighteners. A number of studies have reported a modified cellulose crystallization[4,18–20] with a fluorescent brightener of the diaminostilbene family, Tinopal LPW™ (4,4′-bis[2-hydroxyethylamino-1,3,5-triazin-2-yliamino]-2,2′-stilbenedisulfonic acid, previously sold under another trade name, Calcofluor White™). Haigler *et al.*[4] first demonstrated that cellulose crystallization could be uncoupled from glucan chain polymerization with this dye. Furthermore, they showed that upon washing to remove the dye, cellulose I microfibrils could be formed. In a subsequent study in which higher dye concentrations were employed (> 8 μM), nonmicrofibrillar glucan dye sheets were synthesized by a rough colony variant of *A. xylinum* strain AY 201[18]. These glucan dye sheets (*Figure 2*) have been proposed to exist as non-crystalline (but ordered) glucan sheets, coated on both surfaces with dye molecules, which are helically coiled to produce a three-dimensional tubular structure[21]. Acid washing of the glucan dye sheets also has been shown to remove the dye molecules, allowing cellulose–cellulose interactions to prevail[21]. This leads to the subsequent crystallization into cellulose microfibrils[18,21].

* To whom correspondence should be addressed

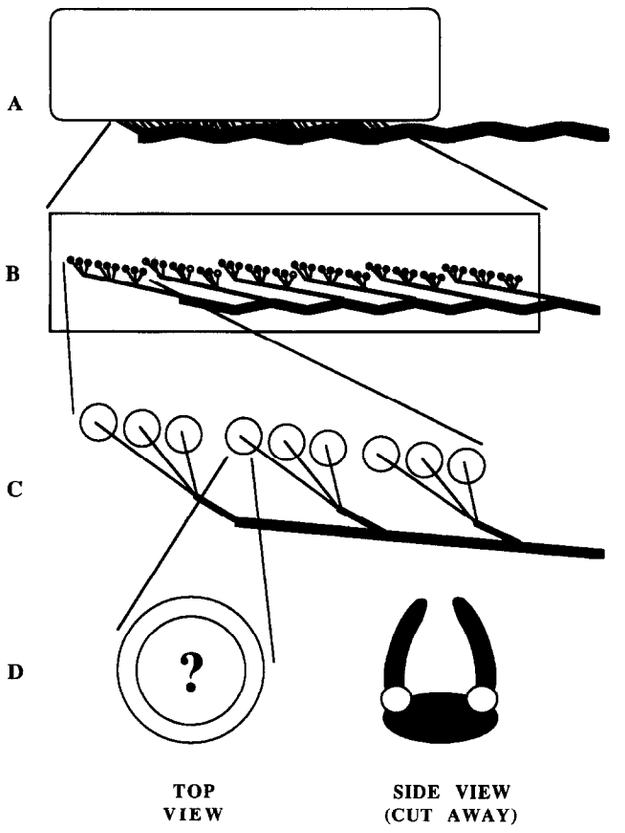

Figure 1 Hierarchical levels of crystallinity in bacterial cellulose. (A) A complete cell of *Acetobacter* (white oblong). The slight zigzag arrangement depicts the twisting of the cellulose ribbon. (B) Detail of A showing the single terminal complex (TC) composed of arrays or clusters of TC subunits. Bundles of microfibrils are shown associated with their respective arrays of TC subunits, illustrated schematically as clusters of nine TC subunits (circles). (C) Detail of B showing one bundle of three microfibrils. Each microfibril requires three TC subunits for its assembly. (D) Detailed views from C showing the single TC subunit in top view (left) and cross-section (right). A single TC subunit has a catalytic region at the base depicted by the grey region in the cross-section view. The channel is formed by transmembrane components, depicted by the white and black structures. These structures, in turn, form the extrusion pore shown by the opening. The minicrystal is assembled at some point in the cavity and is extruded through the pore of the TC subunit (? = the arrangement of the catalytic sites is not known)

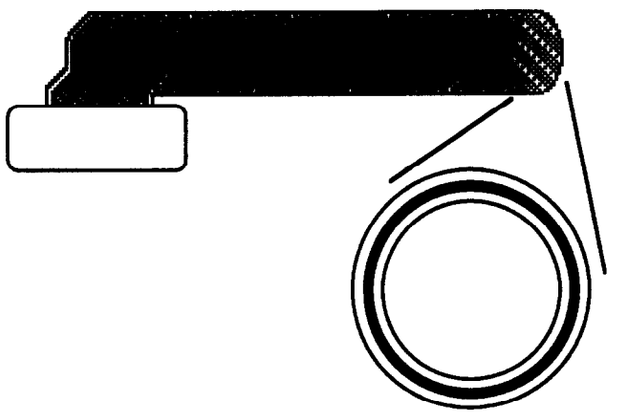

Figure 2 The model of *in vivo* glucan dye sheet formation in *Acetobacter xylinum* as described by Haigler and Chanzy[21]. Tinopal LPW™ is speculated to saturate glucan chains as they are extruded from the TC subunits to form a glucan sheet. The sheet then coils into a closed tube which is coated on both surfaces with dye stacks. The white circles represent dye stacks and the black circle represents a glucan sheet

We are hypothesizing that u.v. irradiation also may induce cellulose microfibrils by the removal of dye molecules. Tinopal LPW™ exists as two isomers. During its transition to the nonplanar *cis* isomer, the planar *trans* isomer absorbs ultraviolet (u.v.) radiation and re-emits light in the visible range (approximately 450 nm)[22]. The nonplanar *cis* isomer does not bind to glucan chains[23]. Such photoisomerization would allow a more precise experimental manipulation of the crystallization process by adjusting the intensity of the u.v. radiation. Thus, the goals of this study have been: (a) to induce a controlled crystallization of the glucan dye sheets by photoisomerization of the dye molecules; (b) to analyse the ensuing dynamic crystallization patterns of cellulose by correlating the video data with electron microscopy; and (c) to determine which crystalline allomorph is produced with X-ray diffraction analysis.

EXPERIMENTAL

Preparation of glucan dye sheets

Resting cells of *A. xylinum* strain AY 201 (ATCC 23769) were prepared by the Celluclast™24 method[6]. A single highly crenate colony (5–9 days) was used to inoculate 100 ml of SH containing 150 μl of filter sterilized Celluclast™. The inoculated solution was incubated for 2 days at 28°C, in the dark on a rotary shaker at 120 rpm. After incubation, the solution was filtered through six layers of cheesecloth to remove undigested cellulose, then centrifuged at 1744 × *g* for 5 min at 4°C. The pellet was washed twice in excess 50 mM sodium phosphate buffer (pH 7.0–7.5) to remove any remaining Celluclast™. The cells were resuspended in approximately 1 ml of 50 mM sodium phosphate buffer (pH 7.0 7.5).

Synthesis of glucan sheets for light and electron microscopy was accomplished by adding 8 μl of resting cell suspension to 152 μl of 250 μM Tinopal LPW™ in Schramm–Hestrin (SH) medium[25] (pH 6.1–6.2). Incubations were carried out for 20 min in droplets on Parafilm™ in the dark at 19°C. For light microscopy, the sample was gently removed from the Parafilm™ and placed on a glass slide for observation. For electron microscopy, the sample was attached to formvar coated copper grids and negatively stained for observation. Larger quantities of glucan dye sheets, referred to here as bulk cultures, were prepared for X-ray diffraction by inoculating 210 ml of incubation solution at a final concentration of 250 μM Tinopal LPW™ with 200 μl of cell suspensions derived by the Celluclast™ method and incubating in the dark for 14–16 h. Longer incubations (> 18 h) were avoided because of the formation of precipitates, even in the absence of cell suspension. While the precipitate could be removed with 0.2% NaOH, glucan dye sheets also were removed by such treatment. Bulk cultures were recovered by centrifugation at 16 300 × *g* for 15 min, washed three times in deionized water, and resuspended in a minimum amount of water.

Induction of cellulose crystallization

Crystallization of glucan dye sheets was induced by irradiating the material with ultraviolet light (365 nm from an OSRAM HBO-100 lamp) with a Zeiss Universal Microscope equipped for epifluorescence microscopy. Samples for video microscopy were irradiated under a

Table 1 Terminology used in this paper to refer to the hierarchy of cellulose crystallization in *Acetobacter xylinum*

Terms used in this paper	Other terms used in cellulose research	Definition
Glucan chain	Cellulose chain[8]	Polymer of β-1,4 linked D cellobiose residues synthesized from a single catalytic site on the cellulose synthase enzyme complex[6]
Minisheet	Cellulose sheet[10] Transient sheet[9] Glucan sheet[11]	Association of a few to several glucan chains by hydrogen bonds and/or van der Waals forces as a single monolayer after extrusion from the catalytic sites but still within a single TC subunit. No direct evidence for this stage. Hypothesized based on several dye altered cellulose studies[18,20,21]. Bonding has been disputed between these studies; however, bonding by van der Waals forces is supported by energy analysis[16]
Minicrystal	Elementary fibril[11] Subfibril[12]	Association of glucan chains from single TC subunit. Theorized to be an aggregation of minisheets. This level can be modelled with molecular mechanics applications
Microfibril	–	Single crystalline entity[14]. Estimated to be comprised of at least 3 minicrystals[12]. In other organisms with low crystallinity cellulose, could be composed of a single minicrystal and thus be equal in such a case
Microfibrillar Bundle	Bundle of microfibrils[12]	Loose association of microfibrils often forming a very relaxed helix. Believed to form by discontinuous arrays within a single linear TC[12]
Ribbon	–	Highest level, loose association of microfibrillar bundles, and the end result of the linear TC arrangement

glass cover slip during observations. The TEM samples, adhered as a wet film on formvar coated copper grids, were irradiated by placing the grids with the sample side up in to the u.v. beam path of the light microscope as specified above. The TEM specimens were irradiated without an objective lens in place (unfocused) as well as with a 32 × Neofluor objective lens whose aperture was fully open (focused). In both cases, the wet surface of the grid was positioned as close to the beam of light as possible. Bulk samples for X-ray diffraction were placed in a quartz cuvette and irradiated in the microscope's u.v. beam path in the unfocused condition for 36–48 h. Irradiation of bulk samples with hand-held u.v. illuminators and u.v. lamps in fume hoods was insufficient for induced crystallization as observed by morphology with TEM, even when employed as long as 168 h.

Glucan dye sheets also were induced to crystallize by treatment with acid, since previous work[21] indicated that this method induces cellulose microfibril formation. Samples for light microscopy were acid washed by wicking 0.25 N HCl under the glass cover slip using capillary action supplied by a Kimwipe™ placed on the opposing side of the cover slip. Samples for electron microscopy were acid washed by slowly allowing droplets of 0.25 N HCl to run over the glucan dye sheets adhering to the EM grids immediately prior to negative staining.

Video microscopy and digital image analysis

Epifluorescence microscopy was linked with real-time video microscopy to analyse the dynamics of the photoisomerization process. A control slide of *Pleurosigma angulatum* punctae spacings with uniform centre-to-centre distance of 0.45 μm[26] was videotaped to calibrate the spatial measurements.

Still frames were photographed from the video monitor using an Olympus OM-2 camera loaded with Kodak Tri-X film (ASA = 400). The photographic images were digitized and stored in the array processor of a Kontron IBAS 1.0 Image Processing Unit (Munich, Germany). Densimetric traces were performed to determine length and width changes of the glucan dye sheets as the dye molecules were photoisomerized, and artificial colours were assigned to the gray scale to determine underlying morphological changes during the induced crystallization process.

Electron microscopy

Samples of glucan dye sheets, the photoisomerized product, and the acid-treated product adhering to formvar coated, 300 mesh copper grids were negatively stained with 2.5% uranyl acetate for observations using a Philips 420 transmission electron microscope (TEM) at 100 kV. Condenser 1 on the TEM was set at spot size 1, with a 150 μm condenser aperture and a 100 μm objective aperture in place.

X-ray powder diffraction analysis

X-ray powder patterns were obtained with a Philips PW 1024/30 Debye Scherrer camera using Ni-filtered CuK_α (1.542 Å) radiation at 35 kV and 25 mA. Samples of bulk glucan dye sheets and photoisomerized bulk glucan dye sheets were observed with TEM prior to preparation for X-ray diffraction. Samples were dried on ethanol cleaned glass slides in the dark for 24–48 h. With clean razor blades, the dried samples were scraped from the slides and packed into 0.3 mm glass capillary pipettes. The X-ray reflections were recorded and compared to

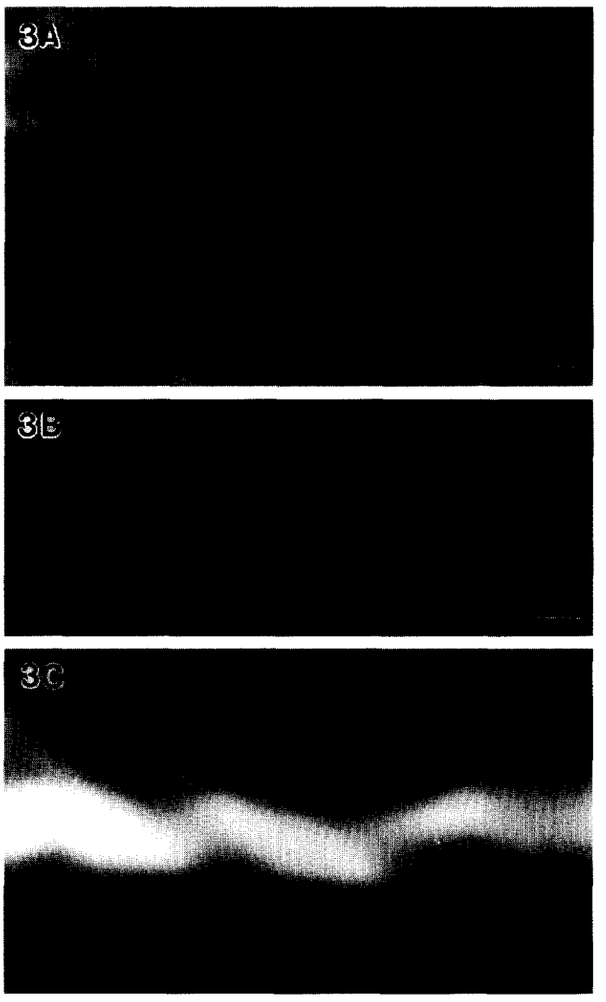

Figure 3 Initial stages of photoisomerization observed with a 40 × PLANAPO objective lens. (A) Note the membranous and sheet-like architecture of the glucan dye sheets visualized with darkfield optics. Bar = 2 μm. (B) With epifluorescence optics, the PLANAPO lens pathway minimizes the amount of u.v. irradiation striking the specimen, thereby preserving the initial stages of crystallization. The shadowing effect introduced by a pseudoplast filter applied during digital image processing emphasizes the helical nature of the glucan dye sheets. Bar = 1 μm. (C) Within the first 2–3 s of minimal exposure to u.v. irradiation, the helical seam of glucan dye sheets breaks (arrows). Bar = 1 μm

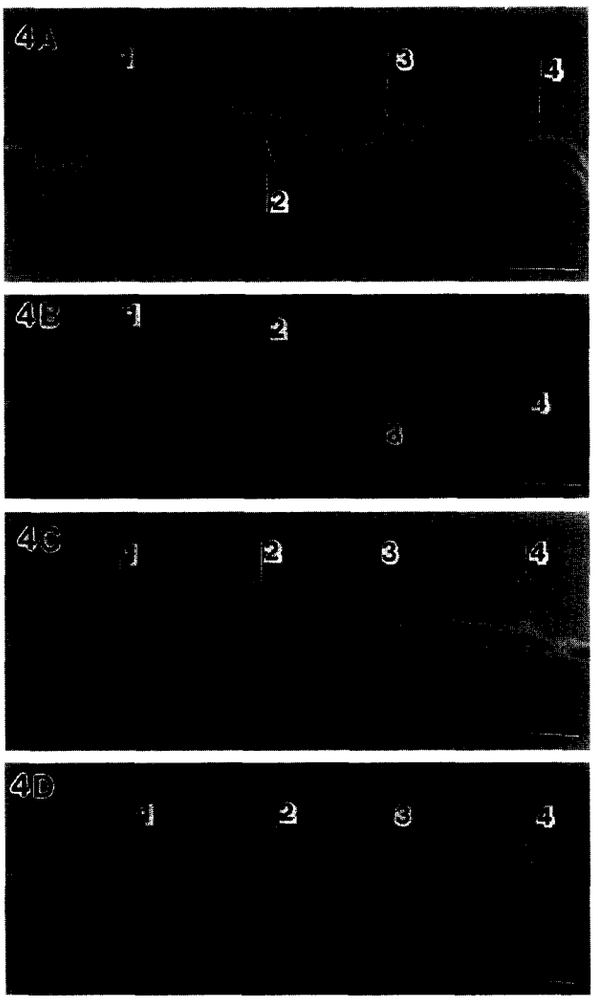

Figure 4 Real-time sequence (30 s) of photoisomerization observed with a 100 × Neofluor objective lens. The design of the Neofluor objective lens shortens the pathlength so that more u.v. irradiation will irradiate the specimen. In this particular glucan dye sheet, the two ends are apparently fixed, allowing for internal marking for dimensional analysis. Note the attachment point at the left where the glucan dye sheet attaches to the cell. Arrows 1 4 indicate respective loci of width measurement depicted in *Figure 5*. (A) At the initiation of the sequence, this particular glucan dye sheet exhibited typical undulations, indicating its flexible character. The initial uncoiling is characterized by the slightly helical orientation of the sheet which was constant enhanced by artificial grey value assignment. (B) After 14 s of u.v. irradiation, the glucan dye sheet began to contract and acquire rigidity. (C) After 26 s, the uncoiling tube eventually became linear due to the contraction process. (D) After 28 s, the uncoiled tube ultimately broke away from the cell and recoiled, apparently due to the strain of contraction. Bars = 2 μm

control samples of bacterial cellulose synthesized in the absence of Tinopal LPW^{TM}.

RESULTS

Video microscopy and digital image analysis

Glucan dye sheets consist of flexible, membranous tubes (*Figure 3A*). The first visible change of glucan dye sheets upon exposure to u.v. irradiation is the appearance of a helical seam as the tubes begin to unwind (*Figures 3B,C*). Real time video analysis revealed that during the photoisomerization process a violent torsional motion of the tube occurs. The flexibility of the collapsing tube appeared to decrease as the tube became more linear and rigid after 30 s of intense u.v. radiation (using a 100 × Neofluor objective lens) (*Figure 4*).

The violent torsional motion as the glucan dye sheets photoisomerized made measurements difficult as the entire sheet was generally never in focus at any given time and different portions of the glucan dye sheets would come in and out of focus during the process. Glucan dye sheets generally appeared to decrease in length. Densimetric trace analysis was performed on one glucan dye sheet (*Figure 4*) that was found to have been fixed to two endpoints (the cell which synthesized it and an unidentified mass in the incubation solution). This analysis indicated that the glucan dye sheet continually decreased in length during the photoisomerization process (*Figure 5*); however, the tube width initially increased, but then soon afterward appeared to decrease (*Figure 6*).

Torsional changes also appeared during acid treatment of glucan dye sheets; however, the rate of dye removal was so much faster than the photoisomerization

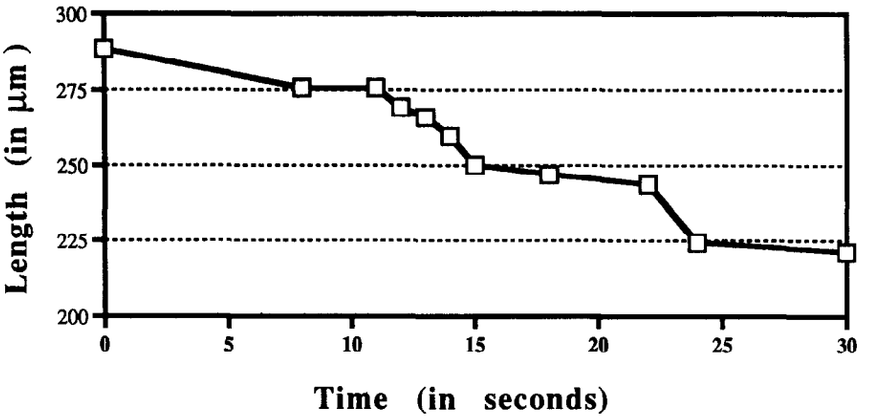

Figure 5 Decrease in glucan dye sheet length during u.v. irradiation. This graph was obtained from a tube observed with two fixed ends illustrated in *Figure 4*

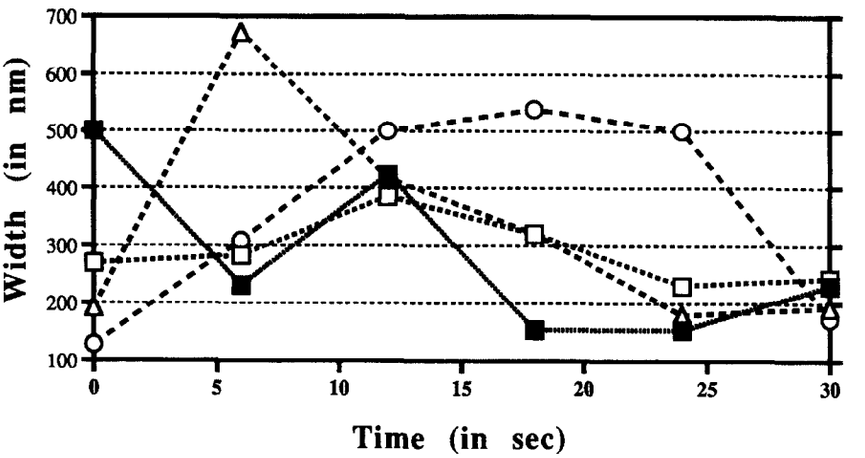

Figure 6 Alteration in glucan dye sheet width during u.v. irradiation. This graph was obtained from the tube observed with two fixed extremities illustrated in *Figure 4*. The tube was measured at four different points between the two extremities and measured at defined time intervals. The general trend observed was an overall initial increase in width followed by a subsequent decrease in width. Point 1 is the only position along the tube where a decrease in width occurs before the initial increase in width. Point 1 was measured near the bacterium and possibly decreased initially due to the strain placed on the tube by the fixed extremity (point 1 = black square; point 2 = white square; point 3 = white triangle; point 4 = white circle)

process that a brilliant fluorescent flash appeared as the acid encountered the glucan dye sheets. Consequently, the video appeared very blurred and details of the crystallization process were lost.

Electron microscopy

Glucan dye sheets consist of single, large tubes each associated with a cell (*Figure 7A*). These tubes extended at a roughly 45° angle to the longitudinal axis of the cell. Although the boundaries of these tubes easily could be detected, the number of folds confounded the measurements of diameter such that only the widest points of each tube were measured (*Table 2*).

After 1 min of focused u.v. radiation (*Figure 7B*), several microfibrils are evident and a background haze of stained material is presumably the remainder of the tubes. After 3 min of focused u.v. radiation, the background haze is greatly reduced (*Figure 7C*), and after 5 min of focused u.v. radiation, the tube completely collapsed into helically oriented microfibrils which associated into small microfibrillar bundles (*Figure 7D*). The helical pitch of the microfibrils ranged from approximately 518 nm to 722 nm (*Table 3*), and several of the microfibrils appeared to have 'cracking loci', points where the helix direction changes sharply rather than gradually. The photoisomerized product ranged in diameter from 209 nm to 232 nm (*Figure 7D*), which is much wider than the 71 nm to 93 nm range typical of the bacterial cellulose ribbon (*Table 2*).

Ten minutes of unfocused u.v. irradiation of the glucan dye sheets led to a photoisomerized product (*Figure 7E*) that was much narrower, ranging from 114 nm to 154 nm (*Table 2*), than the product formed with focused u.v. irradiation. The helical pitch of the microfibrils was much greater and approximated the normal cellulose microfibril helical pitch (*Table 3*) which is often described as twisting of a ribbon[27].

In comparison, acid treatment (*Figure 7F*) produced microfibrils with a pronounced helical orientation (*Table 3*). Microfibrils induced by acid treatment were slightly narrower in width than normal cellulose I microfibrils (*Table 4*), while microfibrils induced by photoisomerization were slighter greater in width (*Table 4*). Furthermore, the standard deviations representing acid treatment data were much narrower than those of the photoisomerization data.

X-ray diffraction analysis and electron microscopy

X-ray powder diffraction of unaltered bacterial cellulose yielded reflections at 2.6 Å, 3.9 Å, and 5.3 Å, and 6.1 Å

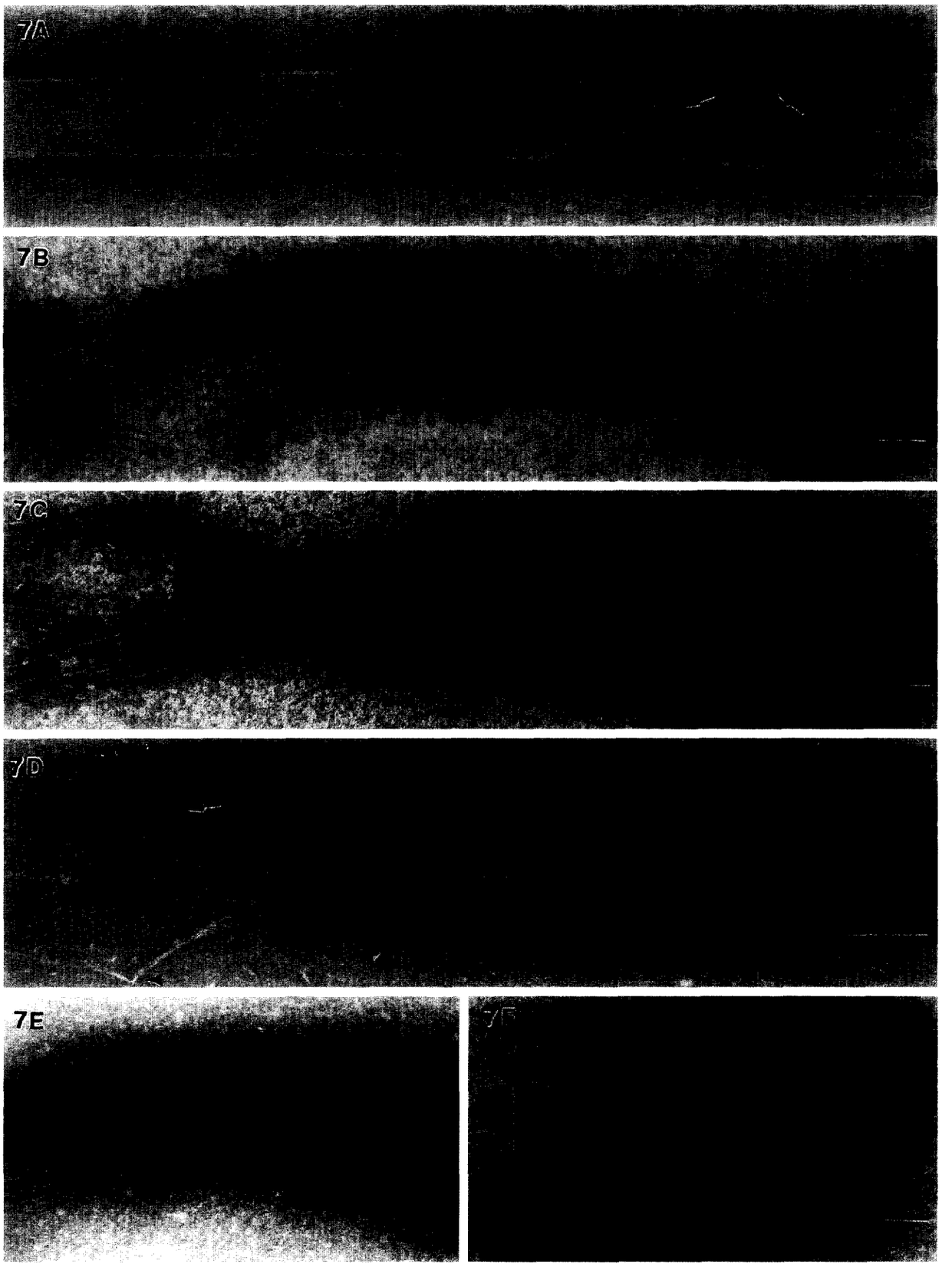

Figure 7 Electron micrographs of glucan dye sheets induced to crystallize into cellulose microfibrils. (A) Glucan dye sheets never exposed to acid washing or u.v. irradiation consist of a single, large extended tube with a helical seam (arrows). (B) After 1 min u.v. irradiation focused with a 32× objective lens, the helical seam appears to have broken and microfibrils begin to appear. (C) After 3 min of focused u.v. exposure, the glucan dye sheet microfibrils predominate. (D) After 5 min of focused u.v. exposure, the glucan dye sheet has crystallized into a distinctive helical arrangement of microfibrils and microfibril bundles (arrows). Also notice the cracking loci (arrowheads) along several of the microfibrils. (E) Glucan dye sheets exposed to 10 min of u.v. irradiation without an objective lens (less intense irradiation) have a similar fibrillar appearance to glucan dye sheets exposed to 5 min of focused u.v.; however, these microfibrils are more extended and exhibit fewer cracking loci. (F) After 5 min of acid treatment, glucan dye sheets crystallized into sharply angled microfibrils. The very faint background stain evident around the microfibrils may be glucan dye sheets that have not crystallized. Bars = 100 nm

Table 2 Diameter variation between glucan dye sheets and the photoisomerized products

Sample	Mean	Standard deviation	Sample size	Range
Control cellulose ribbons[a]	81.0 nm	± 5.2 nm	50	71.2– 94.0 nm
Glucan dye sheets	209.8 nm	±15.6 nm	50	190.5–254.2 nm
5 min acid treatment product	218.6 nm	± 7.8 nm	50	214.3–241.2 nm
5 min photoisomerized product (u.v. w/32X Neofluor obj lens)	217.4 nm	± 8.2 nm	50	209.8–232.3 nm
10 min photoisomerized product (u.v. without obj lens)	136.7 nm	±11.3 nm	50	114.0–154.0 nm

[a] Control celllose ribbons were synthesized from a cell suspension incubated in SH medium in the absence of Tinopal LPW™

Table 3 Helical pitch (length (nm) of one revolution of a microfibril) variation between between microfibrils of cellulose crystallized by different methods

Sample	Mean	Standard deviation	Sample size	Range
Control cellulose microfibrils[a]	1155 nm	±38	50	1043–1276 nm
5 min acid treatment product	481 nm	±13	50	436–524 nm
5 min photoisomerized product (u.v. w/32X Neofluor obj lens)	624 nm	±30	50	518–722 nm
10 min photoisomerized product (u.v. without obj lens)	845 nm	±14	50	805–887 nm

[a] Control cellulose microfibrils were synthesized from a cell suspension incubated in SH medium in the absence of Tinopal LPW™

Table 4 Microfibril width variation of cellulose crystallized by different methods

Sample	Mean	Standard deviation	Sample size	Range
Control cellulose microfibrils[a]	1.6 nm	±0.1 nm	50	1.3–1.9 nm
5 min acid treatment product	1.2 nm	±0.1 nm	50	0.9–1.3 nm
5 min photoisomerized product (u.v. w/32X Neofluor obj lens)	2.1 nm	±0.6 nm	50	1.2–2.7 nm
10 min photoisomerized product (u.v. without obj lens)	1.9 nm	±0.2 nm	50	1.5–2.3 nm

[a] Control cellulose microfibrils were synthesized from a cell suspension incubated in SH medium in the absence of Tinopal LPW™

(*Figure 8A*), characteristic of the expected cellulose I crystalline allomorph. The bulk glucan dye sheets produced a single 3.9 Å reflection (*Figure 8B*). A strong 3.5 Å reflection and weak 3.9 Å and 5.2 Å reflections (*Figure 8C*) were recorded from the photoisomerized bulk glucan dye sheets. Electron microscopy of the control showed typical ribbon morphology (*Figure 8D*). The bulk glucan dye sheets exhibited a sheet-like morphology that is different than that of glucan dye sheets synthesized on a grid (*Figure 8E*). The sheets are much smaller and appear to have collapsed on top of each other, possible due to the centrifugation process. It is difficult to determine whether the many small lines are merely the edges of these smaller sheets or a mass of intertwined filaments. Most likely there are a few small filaments mixed in with collapsed sheets. Observations of the photoisomerized sample established a microfibrillar nature (*Figure 8F*).

DISCUSSION

Photoisomerization-induced crystallization of glucan dye sheets

In this study, photoisomerization has been shown to induce the crystallization of cellulose microfibrils from glucan dye sheets. The rate of induced crystallization seems to affect the perfection of the *microfibril* size and the maintenance of the crystalline hierarchy of the final cellulose product. The slower the rate of dye removal, the more closely the crystalline hierarchy follows *in vivo* cellulose crystallization with regard to the diameter of the photoisomerized product, microfibril density, microfibril helix pitch within the structure, and microfibril bundle formation. Furthermore, the torsional changes could be an expression of the chirality of cellulose as it crystallizes to form the glucan dye sheets. It is well known that glucose and cellulose are chiral molecules[28,29]. With cellulose, this is evidenced by the liquid crystal dynamics and twisting of ribbons which may relieve strain[30]. In the case of dynamic crystallization induced by dye photoisomerization, the release of strain appears to occur during the uncoiling of glucan dye sheets upon u.v. irradiation.

Dynamics of the induced crystallization process

Based on correlation of video and electron microscopy observations, induced crystallization by photoisomerization can be described in three steps (*Figure 9*). The

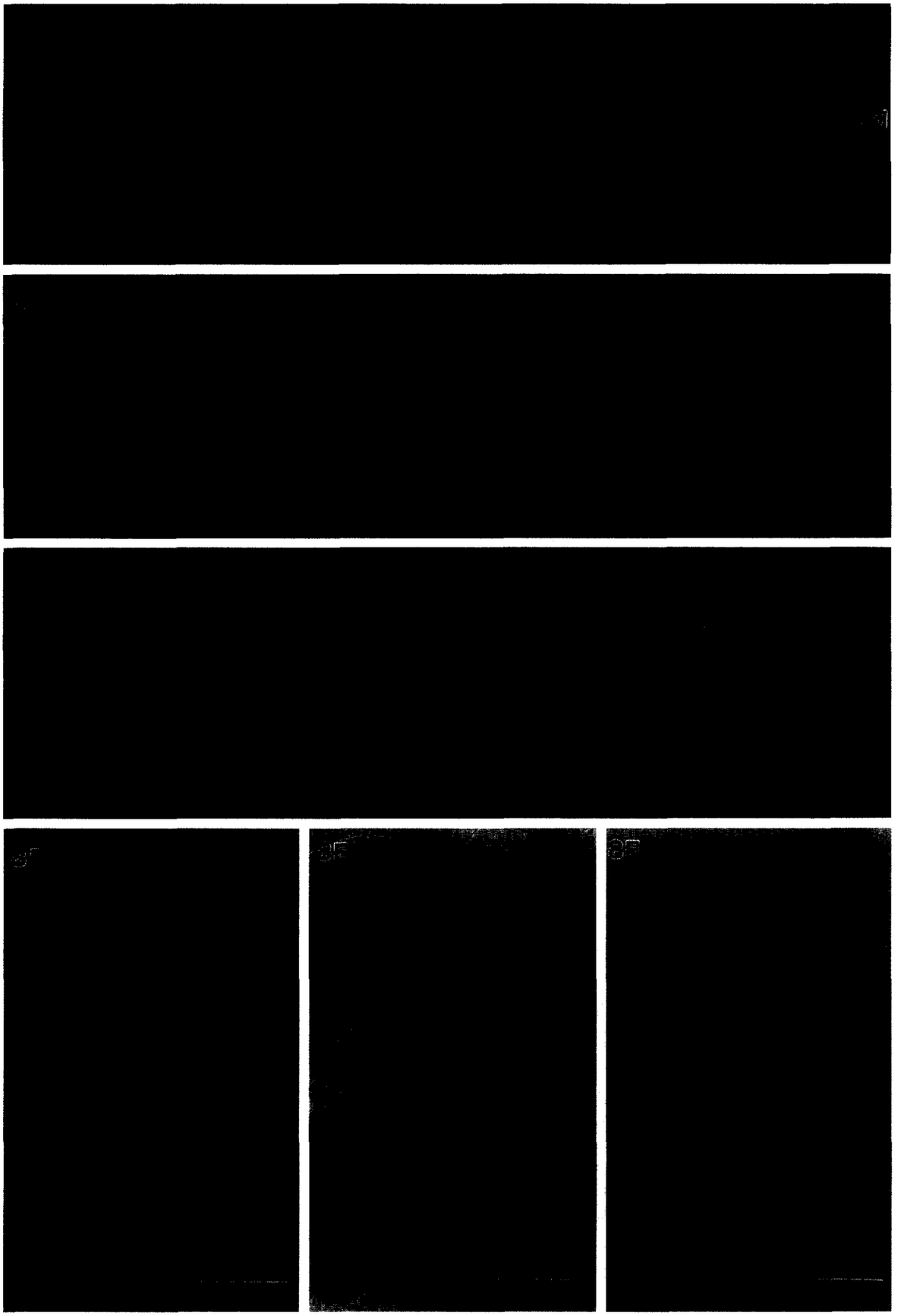

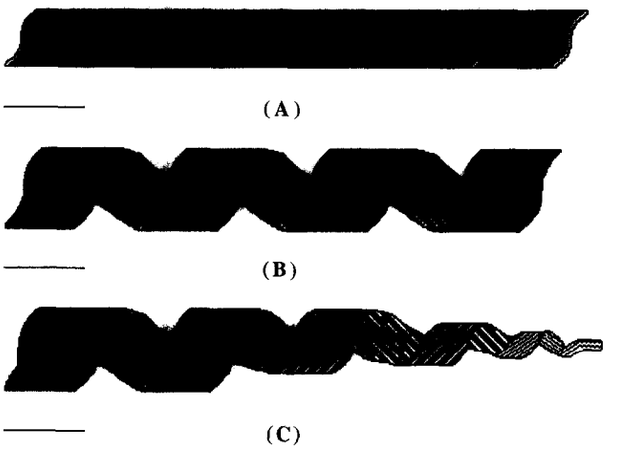

Figure 9 Model for photoisomerization-induced crystallization of glucan dye sheets. (A) As the tube is exposed to u.v., the oriented dye molecules on the outside (indicated by paired white dots) lose their cellulose binding capacity as they photoisomerize, allowing the helical seam to break. (B) The open seam exposes the Tinopal LPW^{TM} on the inside of the tube (indicated by white dots against a grey background) to u.v. irradiation as it uncoils. (C) As more dye molecules are removed from both surfaces, the tube collapses as the sheet folds upon itself by hydrogen bonding to form crystalline microfibrils (indicated by wavy lines in the material at the right)

appearance of a helical seam suggests that the first step in this process is the breaking of the tube along a weak point, the helical seam. The minimal u.v. exposure necessary to break this seam suggests that a high concentration of dye molecules may exist at that site. Once the seam breaks, the tube begins to uncoil, allowing isomerized dye molecules in the interior to be dislodged. Ultimately, the glucan chains crystallize into microfibrils when a critical number of dye molecules bound to a region of the glucan sheet is removed by photoisomerization. The removal of dye molecules would allow interactions between neighbouring glucan chains to prevail. Decreasing the rate of dye removal possibly allows the glucan sheet to uncoil more before all the dye molecules are removed. Microfibrils induced by acid treatment have been postulated to crystallize in a helical orientation because such an orientation corresponds to the organization of the glucan chains in the glucan dye sheet[21]. In the photoisomerization process, decreasing the rate of uncoiling by lowering the intensity of the u.v. has been correlated in this study with a photoisomerized product of greater microfibril helix pitch and a smaller diameter (*Tables 2* and *3*).

Differences in mean microfibril width may be explained by the mechanisms of induced crystallization. As shown in this study and in previous work[21], acid treatment is a chemical means for inducing microfibril formation. As such, it has a global effect. A large mass of dye molecules disassociate all at one time, as evidenced by the brilliant flash of fluorescence. Ensuing crystallization is rapid and leads to narrower microfibrils. This global crystallization results in more uniform microfibril dimensions with a minimal standard deviation. Furthermore, the very faint background stain evident around the microfibrils may be glucan dye sheet that has not crystallized. Photoisomerization, on the other hand, is a physical means for inducing microfibril formation. It has a slower and more localized effect because of the u.v. irradiation refracting and reflecting in the incubation solution. These changes in direction of the u.v. irradiation could result in some areas of glucan dye sheets being irradiated with more intense u.v. while other areas would by receiving less intense u.v. This localization-dependent crystallization leads to a larger variance in microfibril width.

Crystallographic analysis of the photoisomerized product

The localized effect of the photoisomerization induced crystallization may also lead to the formation of a cellulose-dye composite. While photoisomerization does lead to cellulose microfibrils, as indicated by a characteristic morphology and the 3.9 Å and 5.2 Å reflections, these microfibrils exhibit a very strong reflection at 3.5 Å not found in the cellulose I allomorph. Furthermore, the 2.6 Å reflection in typical cellulose I is absent in the photoisomerized product. The absence of this reflection suggests that the cellulose I lattice has been deformed in these induced microfibrils. The presence of a strong 3.5 Å reflection and the variability in the microfibril width (*Table 4*) suggests that dye molecules have become incorporated into the cellulose lattice. If this incorporation takes place, then the microfibrils represent a composite of parallel glucan chains with dye molecules deforming the cellulose lattice. Such a composite structure would not be predicted to give strong cellulose I reflections because of the deformation influence. We believe this composite structure represents a new cellulose allomorph. As with cellulose derivatives, this composite allomorph appears to be dependent on the cellulose crystalline lattice from which it originated. While cellulose derivatives are composed of chemically altered glucan chains, the composite structure of this investigation has arisen by the physical incorporation or association of dye molecules into the cellulose lattice, in which case the glucan chains are unmodified. It is proposed that this composite structure be referred to as cellulose I-Tinopal composite.

Speculation on in vivo *crystallization*

Cells of the AY 201 strain of *Acetobacter* can synthesize glucan dye sheets in high concentrations of Tinopal LPW^{TM}, whereas cells of most other strains, including the commonly studied NQ 5 strain, can only produce fibrillar material extending perpendicularly to the long axis of the cell[31] using the same dye concentration. These two very different cellulose forms suggest that dye molecules may act differentially or at distinct crystallization hierarchical levels within the two strains. We offer three different explanations for the variability in dye interactions with these strains: (a) differences in pore size, (b) changes in the organization of the catalytic sites within the pore structure, or (c) the extrusion pore acts

Figure 8 X-ray diffraction analysis of glucan dye sheets. (A) Powder pattern of unaltered bacterial cellulose as a cellulose I control. (B) Powder pattern of bulk glucan dye sheets exhibiting single 3.9 Å reflection. (C) Powder pattern of photoisomerized bulk glucan dye sheets show weak cellulose reflections and an additional 3.5 Å reflection. (D) Morphology of bacterial cellulose from sample used in (A). (E) Morphology of glucan dye sheets from sample used in (B). Notice the non-microfibrillar nature of the material. (F) Morphology of photoisomerized bulk glucan dye sheets from sample used in (C). Notice the microfibrils. (a = 6.1 Å; b = 5.3 Å; c = 3.9 Å; d = 2.6 Å; e = 5.2 Å; f = 3.5 Å). Bars = 100 nm

as a mechanical constriction site for the existing glucan chains, resulting in changes in the degree of overlap between glucan chains in a mini-crystal.

Photoisomerization of dye associated glucan sheets provides new insight into the process of cellulose microfibril assembly in two *Acetobacter* strains. Knowledge of bonding of glucan chains within a single minisheet could provide additional understanding of cellulose assembly *in vivo*.

ACKNOWLEDGEMENTS

We would like to thank Mr Richard Santos for technical assistance, and Mr Robert Nagy and Mr Daniel R. Cousins for assistance in schematic drawings. We appreciate the extensive reading and critical review of this manuscript by Dr Alfred D. French. Research was supported in part by NASA grant NAG 9-397 and Welch grant #F-1217 to RMB.

REFERENCES

1 Brown, R. M. Jr., Willison, J. H. M. and Richardson, C. L. *Proc. Natl. Acad. Sci. USA* 1976, **73**, 4565
2 Zaar, K. *J. Cell Biol.* 1979, **80**, 773
3 Benziman, M., Haigler, C. H., Brown, R. M. Jr, White, A. R. and Cooper, K. M. *Proc. Natl. Acad. Sci. USA* 1980, **77**, 6678
4 Haigler, C. H., Brown, R. M. Jr and Benziman, M. *Science* 1980, **210**, 903
5 Brown, R. M. Jr in 'Cellulose and Wood: Chemistry and Technology' (Ed. C. Schuerch), John Wiley and Sons, New York, 1989, pp. 639–657
6 Lin, F. C. and Brown, R. M. Jr in 'Cellulose and Wood: Chemistry and Technology' (Ed. C. Schuerch), John Wiley and Sons, New York, 1989, pp. 473–492
7 Zaar, K. *Cytobiologie* 1977, **16**, 1
8 Meyer, K. H. and Mark H. *Ber Dtsch Chem. Ges.* 1928, **61B**, 595
9 Colvin, J. R. in 'Proceedings of the Ninth Cellulose Conference. I. Symposia on Biosynthesis of Cellulose, Structure and Physics of Cellulose, and Chemistry and Utilization of Lignin' (Ed. A. Sarko), John Wiley and Sons, New York, 1982, pp. 25–32
10 Kai, A. and Koseki, T. *Makromol. Chem.* 1985, **186**, 2609
11 Frey-Wyssling, A. and Mühlethaler, K. *Makromol. Chem.* 1963, **62**, 25
12 Haigler, C. H., White, A. R., Brown, R. M. Jr and Cooper, K. M. *J. Cell Biol.* 1982, **94**, 64
13 Brown, R. M. Jr, Kudlicka, K., Cousins, S. K. and Nagy, R. *Amer. J. Bot.* 1992, **79**, 1247
14 Sugiyama, J., Harada, H., Fujiyoshi, Y. and Uyeda, N. *Mokuzai Gakkaishi* 1985, **31**, 61
15 Haigler, C. H. in 'Cellulose Chemistry and Its Applications' (Ed. T. Nevell and S. Zeronian), Ellis Horwood Ltd., Chichester, England, 1985, pp. 30–83
16 Cousins, S. K. and Brown, R. M. Jr *Polymer* 1995, **36**, 3885
17 Kuga, S. and Brown, R. M. Jr in 'Cellulose and Wood: Chemistry and Technology' (Ed. C. Schuerch), John Wiley and Sons, New York, 1989, pp. 677–688
18 Brown, R. M. Jr., Haigler, C. H. and Cooper, K. *Science* 1982, **218**, 1141
19 Itoh, T., O'Neil, R. M. and Brown, R. M. Jr *Protoplasma* 1984, **123**, 174
20 Kai, A. and Xu, P. *Kobunshi Ronbunshu* 1991, **48**, 449
21 Haigler, C. H. and Chanzy, H. *J. Ultrastructure Mol. Structure* 1988, **98**, 299
22 Lewis, G. N., Magel, T. T. and Lipkin, D. *J.A.C.S.* 1940, **62**, 2973
23 Lanter, J. *J. Soc. Dyers Col.* 1966, **82**, 125
24 Distributed by Novo Nordisk Bioindustrials, Inc., Danbury, CT
25 Hestrin, S. and Schramm, M. *J. Biochem.* 1954, **58**, 345
26 Delgado, R. M., Fink, M. J. and Brown, R. M. Jr. *J. Microsc.* 1989, **154**, 129
27 Frey-Wyssling, A. in 'The Plant Cell Wall', Beltz Offsetdruck, Berlin, 1976, pp. 16–21
28 Stoddart, J. F. 'Stereochemistry of Carbohydrates', Wiley-Interscience, New York, 1971, pp. 1–8
29 Ritcey, A. M., Giasson, J., Revol, J.-F. and Gray, D. G. in 'Cellulose and Wood: Chemistry and Technology' (Ed. C. Schuerch), John Wiley and Sons, New York, 1989, pp. 189–205
30 Revol, J.-F., Giasson, J., Guo, J.-X., Hanley, S. J., Harkness, B., Marchessault, R. H. and Gray, D. G. in 'Cellulosics: Chemical, Biochemical, and Material Aspects' (Eds J. F. Kennedy, G. O. Philips and P. A. Williams), Ellis Horwood, New York, 1993, pp. 115–122
31 Venkataramon, K., Fieser, L. F. and Fieser, M. in 'The Chemistry of Synthetic Dyes, Vol. II', Academic Press, New York, 1952